Electric Power Systems Research 83 (2012) 58–65

Contents lists available at SciVerse ScienceDirect

Electric Power Systems Research

journal homepage: www.elsevier.com/locate/epsr

Evaluation of windowed ESPRIT virtual instrument for estimating Power Quality Indices

Reza Zolfaghari[a,*], Yash Shrivastava[b], Vassilios G. Agelidis[c]

[a] Rm 840, Building J03, School of Electrical and Information Engineering, University of Sydney, NSW, 2006 Australia
[b] School of Electrical and Information Engineering, University of Sydney, NSW, 2006 Australia
[c] School of Electrical Engineering & Telecommunications, University of New South Wales, NSW, 2052 Australia

ARTICLE INFO

Article history:
Received 12 May 2011
Received in revised form 9 September 2011
Accepted 12 September 2011
Available online 21 October 2011

Keywords:
Power quality indices
ESPRIT
Welch spectral analysis
Welch cross spectral analysis
Kalman filter
Forgetting factor

ABSTRACT

The use of subspace and *Matrix Algebra* (MA) methods for estimating *Power Quality Indices* (PQIs) as defined by IEEE Std 1459-2010 is relatively new. For this reason there is room for further research about these methods and their efficiency applied to estimating PQIs. This document presents the design of a *Virtual Instrument* (VI) based on modern subspace, MA and *Least Square* (LS) techniques with a *Kalman Filter* (KF) for estimating PQIs. Further we claim that the efficiency of the subspace method is comparable to the Fourier based methods in typical power system analysis. Simulation and experiments are conducted to further compare the performance of this VI with other VI's which do not use the KF. We also compare this VI with VI's that use the classical *Fast Fourier Transform* (FFT) based method of estimation.

1. Introduction

Power Quality (*PQ*) is an important issue in electricity distribution networks due to the emergence of new systems and technologies. PQ detection is an essential and initial step towards the repair of any fault in the *Power System* (PS) network. This said modern PS such as smart grid systems requires a high level of reliability in their operation [1]. Further the use of modern electrical equipment such as PCs, laser printers and laptops has made PQ issues such as voltage sags and swells to become important PQ events.

There are various sources and reasons for the existence of PQ issues. Renewable energy sources such as wind power can cause PQ problems in the electricity distribution network [2,3]. The increasing use of power switched devices such as laptops, PCs and monitors cause harmonic and other PQ issues on the consumer side of the power network [4]. Moreover voltage sags are mainly caused by power system faults [5] and/or transformer in rush currents [6]. Phase and magnitude imbalances can occur due to single-phase conditioning or load unbalance [7].

IEEE Std 1459-2010 [8] provides definitions and equations for calculating various *Power Quality Indices* (PQIs). Moreover standards such as IEEE Std 1159 [9] or IEEE Std 519 [10] and part 3 of the IEC 61000 standard [11–13], provide useful limits on the levels of harmonics and noise that should be detected in the *Power System* (PS). IEEE Std 1459-2010 is a standard that provides definitions for PQIs to help manufacturers of PQ meters.

The Fourier based technique and the associated *Fast Fourier Transform* (FFT) techniques have and are still being used extensively in the PS literature. They are well known for their robustness towards noise and efficient computational speed. FFT methods are used for detecting transients [14], inter harmonics [15] and harmonic components [16]. However they suffer from leakage [17,18] and picket fencing problems which in turn can cause pseudo aliasing in the FFT spectrum when extracting frequency information from limited number of samples [15,16]. To overcome these problems researchers have tried to make it more robust introducing interpolation functions for estimating a more accurate FFT [15,16,19] or other techniques for getting rid of the leakage [20]. These techniques increase the accuracy of measurements but come with the cost of adding to the computations. Further they mainly target the picket fencing problem and the leakage issue remains unsolved in many of the publications.

* Corresponding author. Tel.: +61 2 9351 4135.
E-mail addresses: re.zolfaghari@gmail.com, reza.zolfaghari@sydney.edu.au (R. Zolfaghari), yash.shrivastava@sydney.edu.au (Y. Shrivastava), vassilios.agelidis@unsw.edu.au (V.G. Agelidis).

0378-7796/$ – see front matter © 2011 Elsevier B.V. All rights reserved.
doi:10.1016/j.epsr.2011.09.009

In modern data collection systems it might be required to detect PQ problems with fewer power signal (i.e. 50 Hz) cycles. The FFT methods, usually due to the use of windows are limited in their accuracy by the *Windowing Technique* (WT) used. A minimum number of cycles in the power system signal need to be observed to get enough accuracy in the detection of phase and magnitude information as well as for estimating the PQIs [21,22].

Modern subspace methods such as *Estimation of Parameters via Rotational Invariance Techniques* (ESPRIT) [23,24] and *Multiple Signal Classification* (MUSIC) [25] are superior as they do not suffer from leakage or picket fencing issues that FFT suffers and usually do not require long observations of the power signal. For this reason they can be used to measure PQ events rapidly even in the presence of a non stationary signal. They have further gained attention in the PS literature and research [26–31]. The publications available in the technical literature have mainly focused on estimating magnitude and frequency information for harmonics [26,29–31], or estimating the oscillatory or damping factor [27] while others have examined the detection of inter-harmonics [28] for PSs. However the use of subspace methods for calculating the PQIs is relatively rare in the technical literature.

In [32] the authors presented a VI for calculating the PQIs using the ESPRIT and *Matrix Algebra* (MA) methods. This document enhances that publication by (a) providing more insight into the computational cost of the subspace based methods compared to the FFT based methods, (b) introducing a new VI for estimating the PQIs by adding a *Kalman Filter* (KF) with a *Forgetting Factor* (FF) to the VI in [32], (c) examining/testing important PQIs from IEEE Std 1459-2010 and (d) comparing the ESPRIT-MA methods VI to the FFT based methods for the VI. More specifically the FFT based methods use the *Welch Spectral and Cross Spectral Analysis techniques* (WSA-WCSA) which are discussed in [21,22]. These techniques require some sort of a window applied to the signal beforehand [33].

In Section IV in [21] we showed how to calculate the PQIs using WSA-WCSA with the help of the FFT method. This document would not repeat the theory presented over there, and refers the readers to that publication. It might be good to point that *Windowing Techniques* (WTs) used in WSA-WCSA and suitable for PQI estimation according to IEEE Std 1459 were initially discussed in [21,22] and are further examined in a concurrent paper.

The organization of this paper will be as follows, the next section would provide some theory on the *Least Square* (LS) ESPRIT and *Total Least Square* (TLS) ESPRIT followed by some MA methods to calculate the amplitude and phase angle of the harmonic components. Following this we present the design of the new VI in Section 3. Some explanation on the performance of the ESPRIT-MA based VI compared to the FFT based WSA-WCSA method is given in Section 4. Important PQIs are formulated and explained in Section 5. Simulation results comparing the computational cost of the VI using the WSA-WCSA method to the VI using the ESPRIT-MA based methods is presented in Section 6. In Section 7 we present the experimental setup to examine the accuracy of the systems compared to one another. In Section 8 we give some discussion on the results and the suitability of these methods to be implemented in real time. We conclude the paper in Section 9.

2. Signal processing techniques

2.1. ESPRIT

In this section we explain the ESPRIT method using the *Autocorrelation Matrix* (AM) which is different from the one presented in [34] which works on the augmented data matrix. The AM behaves as a filter for the ESPRIT method making it more robust towards noise. Following shows the theory of the ESPRIT method calculated in this fashion.

The ESPRIT technique is best suited for complex sinusoids with additive white noise. This can be modeled as:

$$v[n] = \sum_{l=1}^{K} A_l e^{j\Omega_l n} + w[n] \tag{1}$$

where the angular frequencies Ω_l are distinct and satisfy $-\pi < \Omega_l < \pi$, and

$$E\left\{w[k]\right\} = 0 \tag{2}$$

$$E\{w[k]\overline{w[n]}\} = \begin{cases} \sigma_w^2 & \text{for } k = n \\ 0 & \text{otherwise} \end{cases} \tag{3}$$

If we define an $m \times 1$ vector signal $\boldsymbol{y}[n]$ as

$$y[n] = [\, v[n] \quad v[n+1] \quad \cdots \quad v[n+m-1] \,]^T \tag{4}$$

then it can be expressed in vector form in terms of its components as follows:

$$\boldsymbol{y}[n] = \underbrace{\begin{bmatrix} 1 & 1 & \cdots & 1 \\ e^{j\Omega_1} & e^{j\Omega_2} & \cdots & e^{j\Omega_K} \\ \vdots & \vdots & \vdots & \vdots \\ e^{j\Omega_1(m-2)} & e^{j\Omega_2(m-2)} & \cdots & e^{j\Omega_K(m-2)} \\ e^{j\Omega_1(m-1)} & e^{j\Omega_2(m-1)} & \cdots & e^{j\Omega_K(m-1)} \end{bmatrix}}_{V} \underbrace{\begin{bmatrix} A_1 e^{j\Omega_1 n} \\ A_2 e^{j\Omega_2 n} \\ \vdots \\ A_K e^{j\Omega_K n} \end{bmatrix}}_{s[n]} + \begin{bmatrix} w[n] & w[n+1] & \ldots\ldots & w[n+m-2] & w[n+m-1] \end{bmatrix}^T \tag{5}$$

The auto correlation of a periodic vector signal corrupted by noise is defined as:

$$\boldsymbol{R}_{yy}[n] = \lim_{N\to\infty} \frac{1}{N} \sum_{k=0}^{N-1} E\{\boldsymbol{y}[k]\boldsymbol{y}^H[k-n]\} \tag{6}$$

The expectation value $E\{\cdot\}$ is taken due to the randomness in our signal because of the noise; if the noise did not exist then E would not have been necessary. Using (5) and (6) the zero lag autocorrelation can be written as [32]:

$$\boldsymbol{R}_{yy}[0] = \boldsymbol{V} \underbrace{\begin{bmatrix} |A_1|^2 & 0 & \cdots & 0 \\ 0 & |A_2|^2 & \cdots & 0 \\ \vdots & \vdots & \vdots & \vdots \\ 0 & 0 & \cdots & |A_K|^2 \end{bmatrix}}_{D} \boldsymbol{V}^H + \sigma_w^2 \boldsymbol{I}_m \tag{7}$$

Since practically we cannot observe the signal for infinite duration we have to estimate (7) over a finite window length

$$X = \begin{bmatrix} v[0] & v[1] & \cdots & v[M-m] \\ v[1] & v[2] & \cdots & v[M-m+1] \\ \vdots & \vdots & \vdots & \vdots \\ v[m-1] & v[m] & \cdots & v[M-1] \end{bmatrix} \tag{8}$$

$$\hat{R}_{yy}[0] = \frac{1}{(M-m)}(X^H)(X)$$

In our scheme we follow the procedure by estimating (7) using (8).

Being a Hermitian matrix $\boldsymbol{R}_{yy}[0]$ has an eigen decomposition of the following form:

$$\boldsymbol{R}_{yy}[0] = \boldsymbol{U}\boldsymbol{\Lambda}\boldsymbol{U}^H \tag{9}$$

We can assume that the eigen values are in decreasing order. Also the unitary matrix $\boldsymbol{U}$ is formed from two sub matrices one belonging to the signal subspace and the other belonging to the noise subspace

$$\boldsymbol{U} = [\underbrace{\boldsymbol{U}_s}_{m\times K} \quad \underbrace{\boldsymbol{U}_w}_{m\times(m-K)}] \tag{10}$$

From (9) and (10) it can be realized that

$$\boldsymbol{R}_{yy}[0] = \boldsymbol{U}\boldsymbol{\Lambda}\boldsymbol{U}^H = [\,\boldsymbol{U}_s \quad \boldsymbol{U}_w\,]\begin{bmatrix}\Lambda_s & 0\\ 0 & \Lambda_w\end{bmatrix}\begin{bmatrix}\boldsymbol{U}_s^H\\ \boldsymbol{U}_w^H\end{bmatrix}$$
$$= \boldsymbol{U}_s\Lambda_s\boldsymbol{U}_s^H + \boldsymbol{U}_w\Lambda_w\boldsymbol{U}_w^H \tag{11}$$

where Λ_s and Λ_w are diagonal matrices corresponding to eigen values belonging to the signal subspace and the noise subspace respectively. If we denote the first $(m-1)$ rows of $\boldsymbol{U}_s$ as $\boldsymbol{U}_{s1}$ and the last $(m-1)$ rows of it as $\boldsymbol{U}_{s2}$ It can be shown that $\boldsymbol{V}_1 = \boldsymbol{U}_{s1}\boldsymbol{T}$ and $\boldsymbol{V}_2 = \boldsymbol{U}_{s2}\boldsymbol{T}$. From the structure of $\boldsymbol{V}$ we have:

$$\boldsymbol{V}_2 = \boldsymbol{V}_1\boldsymbol{\Phi} \tag{12}$$

where $\boldsymbol{\Phi}$ is defined as:

$$\boldsymbol{\Phi} = \begin{bmatrix} e^{j\Omega_1} & 0 & \cdots & 0\\ 0 & e^{j\Omega_2} & \cdots & 0\\ \vdots & \vdots & \vdots & \vdots\\ 0 & 0 & \cdots & e^{j\Omega_K}\end{bmatrix} \tag{13}$$

Since $\boldsymbol{\Phi}$ and $(\boldsymbol{U}_{s1}^H\boldsymbol{U}_{s1})^{-1}\boldsymbol{U}_{s1}^H\boldsymbol{U}_{s2}$ are similar matrices [32]. For the *Least Square* (LS) ESPRIT we can evaluate the eigen values of $\boldsymbol{\Phi}$ (i.e. $e^{j\Omega_1}, e^{j\Omega_2}, \ldots$) from the eigen values of [32]:

$$(\boldsymbol{U}_{s1}^H\boldsymbol{U}_{s1})^{-1}\boldsymbol{U}_{s1}^H\boldsymbol{U}_{s2} \tag{14}$$

The other method for finding the ESPRIT algorithm is the TLS-ESPRIT to find the *Total Least Square* (TLS) [35] we need to compute the SVD of the matrix, $\boldsymbol{U}$ [36]:

$$\boldsymbol{U} = \boldsymbol{S}_U\boldsymbol{\Lambda}_U\boldsymbol{U}_U \tag{15}$$

the matrix $\boldsymbol{U}_U$ can be decomposed into the form

$$\boldsymbol{U}_U = \begin{bmatrix}\boldsymbol{U}_{U1} & \boldsymbol{U}_{U2}\\ \boldsymbol{U}_{U3} & \boldsymbol{U}_{U4}\end{bmatrix} \tag{16}$$

The TLS-ESPRIT is obtained by finding the eigen values of:

$$\boldsymbol{U}_{U2}(\boldsymbol{U}_{U4})^{-1} \tag{17}$$

which gives a TLS estimate to the eigen values of the matrix $\boldsymbol{\Phi}$ (i.e. $e^{j\Omega_1}, e^{j\Omega_2}, \ldots$). Finally the angular frequencies can be found taking the inverse natural logarithmic function of $\boldsymbol{\Phi}$.

2.2. MA for finding phase and magnitude information

Once the angular frequencies are found using the above methods of LS-ESPRIT or TLS-ESPRIT we can find the amplitude for our harmonic components using the relation from (7):

$$\boldsymbol{D} = (\boldsymbol{V}^H\boldsymbol{V})^{-1}\boldsymbol{V}^H\boldsymbol{R}_{yy}[0]\boldsymbol{V}(\boldsymbol{V}^H\boldsymbol{V})^{-1} - \sigma_w^2(\boldsymbol{V}^H\boldsymbol{V})^{-1} \tag{18}$$

Further a least square estimate for the phase information can be found using the relation in (5):

$$\hat{\boldsymbol{s}}[n] = (\boldsymbol{V}^H\boldsymbol{V})^{-1}\boldsymbol{V}^H\boldsymbol{y}[n]$$
$$\Rightarrow \begin{bmatrix}\hat{A}_1 & \hat{A}_2 & \cdots & \hat{A}_K\end{bmatrix}^T \tag{19}$$
$$= (\boldsymbol{\Phi}^n)^H(\boldsymbol{V}^H\boldsymbol{V})^{-1}\boldsymbol{V}^H\boldsymbol{y}[n]$$

Stage 1 and 2 of the following flowchart summarizes the above procedure for finding the frequency, magnitude and phase information.

2.3. KF with FF

KF are very useful when trying to extract a quantity from measurements corrupted by random variations. Every KF contains a set of equations to predict the state of a variable or a vector and a set of equations for updating them. A state space model for many discrete systems can be modeled as:

$$\begin{aligned}\boldsymbol{x}(d+1) &= \boldsymbol{A}\boldsymbol{x}(d) + \boldsymbol{B}\boldsymbol{u}(d) + \boldsymbol{v}(d)\\ \boldsymbol{y}(d) &= \boldsymbol{C}\boldsymbol{x}(d) + \boldsymbol{s}(d)\end{aligned} \tag{20}$$

where $\boldsymbol{x}(d)$, is our state vector, $\boldsymbol{A}$ is the state transition matrix, $\boldsymbol{u}(d)$ is the input or control vector, $\boldsymbol{B}$ is the input matrix, $\boldsymbol{v}(d)$ is process noise, $\boldsymbol{C}$ is output matrix and $\boldsymbol{s}(d)$ is measurement noise.

Since each of our PQIs are scalar variables we use a simplified version of (20) for the purpose of our KF design. It is good to point that we could indeed assign a vector for all the PQIs that we are trying to filter, and formulate our KF in vector notation, however since the PQIs are independent from each other it is easier to look at them in terms of a scalar value. Let $x[d]$ denote the quantity being computed for the frame d (i.e. any *Power Quality Index* (PQI)). Then our KF assumes that $x[d]$ is constant over the successive frames but the measurements of it ($y[d]$) are affected by a measurement noise $s[d]$ having a Gaussian distribution, i.e.

$$x[d+1] = x[d] \tag{21}$$

$$y[d] = x[d] + s[d] \tag{22}$$

This said, our KF provides a smoothed estimate $\hat{x}[d]$ of $x[d]$ from the measurements according to

$$\hat{x}[d+1] = \hat{x}[d] + \left(\frac{p[d]}{p[d]+R}\right)(y[d] - \hat{x}[d]) \tag{23}$$

Here R denotes the variance of measurement noise and $p[d]$ denotes the optimal variance of the current estimation error $(x[d] - \hat{x}[d])$ which is updated as

$$p[d+1] = \left(\frac{p[d]}{p[d]+R}\right)\alpha R \tag{24}$$

Note that (24) includes the forgetting factor $\alpha \geq 1$ and $p[d]$ eventually converges to a value of $(\alpha-1)R$. The normal KF corresponds to the case of $\alpha = 1$ (and thus $p[d] \to 0$ in steady state) where it can be seen from (23) that the new measurements become gradually less and less important and are eventually ignored completely and the filter is turned off. On the other hand, for very large values of $p[d]$ in (24) (which would be the case for large values of α relative to R), we have $\hat{x}[d+1] \approx y[d]$ and the past estimates (and thus measurements) are ignored. In our implementation we would actually tune α from a large value when the error $(y[d] - \hat{x}[d])$ is large and make it close to 1 once the error gets small to reduce the effect of noise in steady state.

3. Design of the new VI with the added KF

Once the PQI are computed as detailed in section IV of [32] the KF described above is performed on the PQI to reduce fluctuations in the estimation of the index due to the presence of noise or other artefacts such as misalignment of the window with the period of the signal or the presence of inter-harmonics.

In the design of the KF with a FF described in Section 2.3 above we tuned the KF such that when the observation into the KF was significantly different to the estimation out of the KF, α would be assigned a large number. This ensures quick convergence to the actual PQI value. This said when the value of α is large the smoothing in the signal accordingly degrades. On the other hand when our estimate is close enough to the observation, we tune α to be

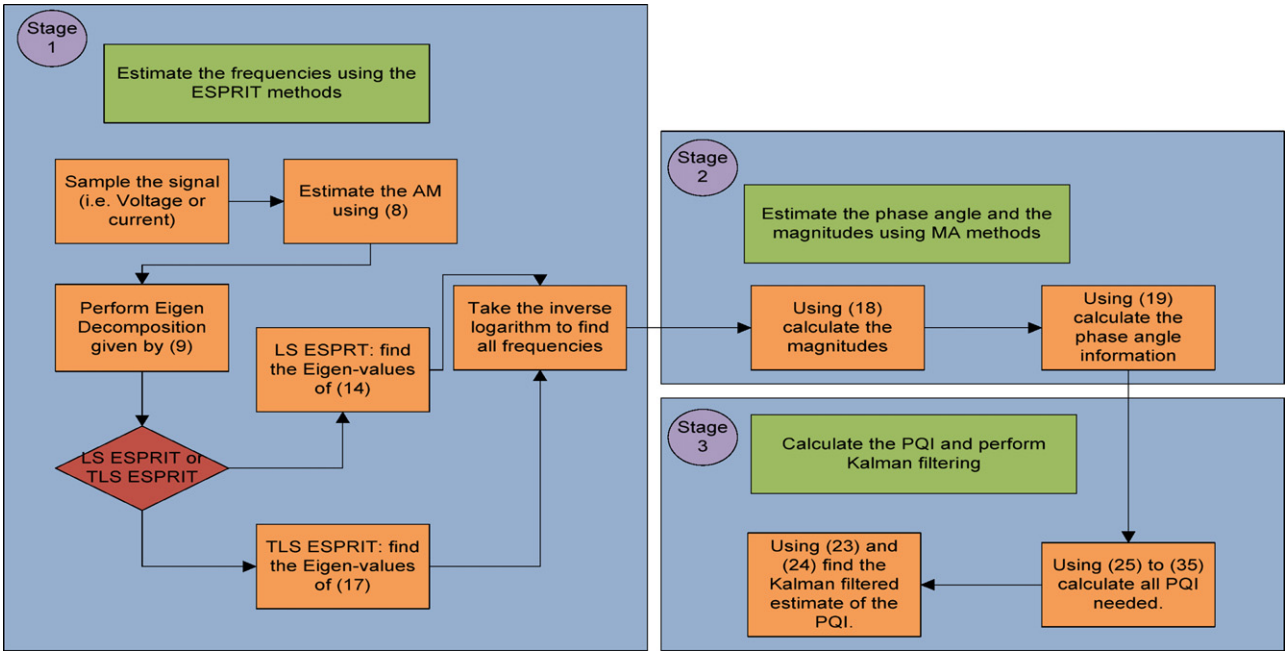

Fig. 1. Flow chart for the ESPRIT-MA method with KF.

small so that we can enjoy proper filtering of the noise. This process requires some knowledge of the system before hand in order to set α to the correct value. Hence the decision for setting α from a large value to a small one is different and depends on the range of the value we are trying to estimate, in the case of our discussion here the approximate range of the PQIs. The VI that uses this KF will be called KF VI in this document. Fig. 1 shows the full design for both VIs.

4. Performance of ESPRIT-MA based methods compared to WSA-WCSA

4.1. Autocorrelation matrix size

It was explained in [32] that the autocorrelation of the sampled signal contains complex terms, some of them with typically low frequencies. These low frequency terms are equal to the difference in the frequencies of adjacent frequency components in the observed signals, frequency spectrum. These terms average to zero if the data length is very long or if the auto-correlation is performed over their period (the smaller the frequency difference is, the bigger the period required).

Further it was stated in [26,32] that the *Autocorrelation Matrix Size* (AMS) plays an important role in the accuracy of the ESPRIT-MA method. It was shown in [26] that there is an optimal size for the AMS. The graphs in Figs. 2 and 3 show the *Percentage Error* (PE) in estimating harmonic magnitude and phase components using the two popular ways of calculating the ESPRIT technique namely LS-ESPRIT and TLS-ESPRIT [37]. It can be seen that detecting more harmonic components requires a larger AMS. Generally a good estimation of the magnitude and phase angle can be achieved if the AMS is bigger than $>2p+c$ where p is the number of real harmonics (i.e. not exponential) and the constant c depends on the number of harmonics and the noise level of the system. Through our simulation and with prior knowledge of PSs we found that for harmonics up to harmonic No. 21, $c=4$ can provide a good estimate in the PS. Hence the AMS needs to be bigger than $>2p+4$ to obtain accurate results for magnitude and phase information. Figs. 2 and 3 show the validity of this statement. This will further be discussed in the coming sections.

4.2. Computation cost of ESPRIT-MA vs. WSA-WCSA

The core computation involved in WSA-WCSA is the calculation of the FFT. It is well known that the FFT method is very efficient in calculating the *Discrete Fourier Transform* (DFT) of a signal. The computational cost of the FFT method is of $O(N\log(N))$ [36] where N is the length of our window in number of samples. The ESPRIT-MA method on the other hand requires the computation of the *Singular Value Decomposition* (SVD) of the *Autocorrelation Matrix* (AM) which is of order $O(n^3)$ [35], where n is the number of rows in our AM.

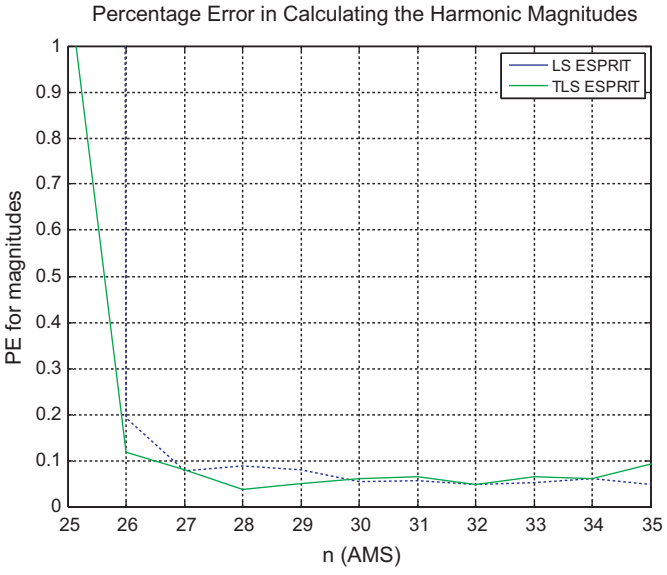

Fig. 2. PE in estimating harmonic magnitudes for LS and TLS ESPRIT versus AMS.

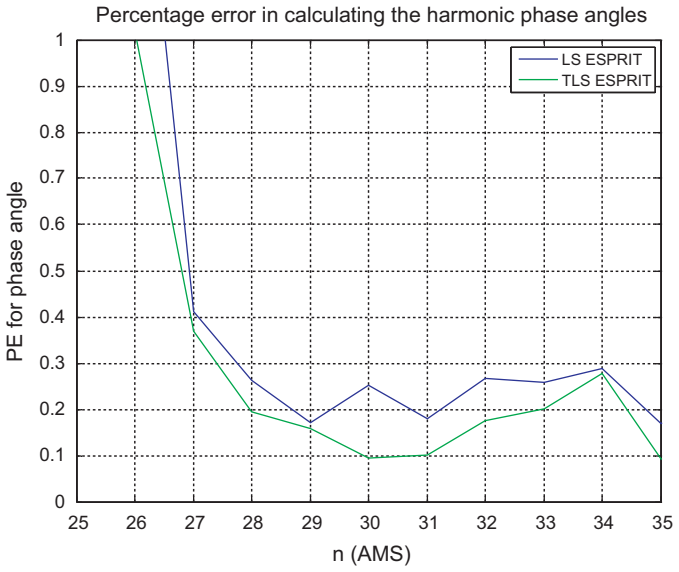

Fig. 3. PE in estimating harmonic phase angles for LS and TLS ESPRIT versus AMS.

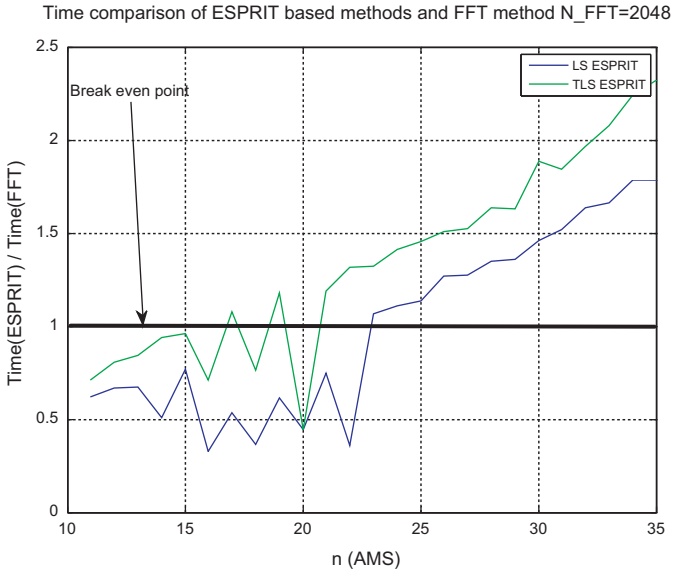

Fig. 4. Computational cost of LS ESPRIT and TLS ESPRIT versus FFT for N_FFT = 2048.

With this knowledge we can realize that for relatively small sizes of the AMS our ESPRIT-MA method can be comparable in computational cost to the FFT based WSA-WCSA method. Fig. 4 shows the time for computing harmonic components using the ESPRIT-MA technique in comparison to the WSA-WCSA/FFT based technique using a 2048 point FFT.

5. Power Quality Indices

IEEE Std 1459 provides many PQIs for measuring PQ. It provides a good insight by breaking the power, voltage and current into fundamental and non fundamental components. In Section III of [21,32] we discussed some of the PQIs in IEEE Std 1459-2010 and how they can be written in component form. Further explanations for some of the most important PQIs are given below.

The concept of effective voltage and current is important in understanding the PQIs defined in the IEEE standard. It is based on the idea of power dissipated on an active load connected as a Y configuration and the rest of the power dissipated on an active load consisting of a Δ (delta) connection. In order to derive later indices we require the effective current and voltage in terms of the measurements given from the sliding window. Further we will be using symmetrical components to define some of the indices by transforming the voltage and current phasors into positive ($\boldsymbol{V}_h^+ = V_h^+ e^{j\theta_h^+}$), negative ($\boldsymbol{V}_h^- = V_h^- e^{j\theta_h^-}$), and zero-sequence ($\boldsymbol{V}_h^0 = V_h^0 e^{j\theta_h^0}$) components as follows (please note ϕ is used for the current phase and θ for voltage phase):

$$\begin{bmatrix} \boldsymbol{V}_h^+ \\ \boldsymbol{V}_h^- \\ \boldsymbol{V}_h^0 \end{bmatrix} = \frac{1}{3} \begin{bmatrix} 1 & e^{j2\pi/3} & e^{j4\pi/3} \\ 1 & e^{j4\pi/3} & e^{j2\pi/3} \\ 1 & 1 & 1 \end{bmatrix} \begin{bmatrix} \boldsymbol{V}_{ah} \\ \boldsymbol{V}_{bh} \\ \boldsymbol{V}_{ch} \end{bmatrix}$$

The symmetric components of the current phasor can be defined in a similar fashion $\boldsymbol{I}_h^+ = I_h^+ e^{j\phi_h^+}$. With this knowledge the effective current can be defined in terms of its harmonic components as follows:

$$I_e^2 = \frac{\left(\sum_{k=1}^{\infty} I_{ak}^2 + \sum_{k=1}^{\infty} I_{bk}^2 + \sum_{k=1}^{\infty} I_{ck}^2 + \sum_{k=1}^{\infty} I_{nek}^2\right)}{3} \tag{25}$$

If we require the fundamental effective current it will be written as:

$$I_{e1}^2 = \frac{(I_{a1}^2 + I_{b1}^2 + I_{c1}^2 + I_{ne1}^2)}{3} \tag{26}$$

Similarly we can define the effective voltage in terms of the harmonic components as:

$$\begin{aligned} V_e^2 = {} & \frac{\sum_{h=1}^{\infty}(V_{ah}^2 + V_{bh}^2 + V_{ch}^2)}{6} \\ & + \frac{\sum_{h=1}^{\infty}(V_{ah}^2 + V_{bh}^2 - 2V_{ak}V_{bh}\ \cos(\theta_{ah} - \theta_{bh}))}{18} \\ & + \frac{\sum_{h=1}^{\infty}(V_{bh}^2 + V_{ch}^2 - 2V_{bh}V_{ch}\ \cos(\theta_{bh} - \theta_{ch}))}{18} \\ & + \frac{\sum_{h=1}^{\infty}(V_{ch}^2 + V_{ah}^2 - 2V_{ch}V_{ah}\ \cos(\theta_{ch} - \theta_{ah}))}{18} \end{aligned} \tag{27}$$

Again if we require the fundamental component of the effective voltage it can be written as:

$$\begin{aligned} V_{e1}^2 = {} & \frac{(V_{a1}^2 + V_{b1}^2 + V_{c1}^2)}{6} + \frac{(V_{a1}^2 + V_{b1}^2 - 2V_{a1}V_{b1}\ \cos(\theta_{a1} - \theta_{b1}))}{18} \\ & + \frac{(V_{b1}^2 + V_{c1}^2 - 2V_{b1}V_{c1}\ \cos(\theta_{b1} - \theta_{c1}))}{18} \\ & + \frac{(V_{c1}^2 + V_{a1}^2 - 2V_{c1}V_{a1}\ \cos(\theta_{c1} - \theta_{a1}))}{18} \end{aligned} \tag{28}$$

Active Power (ACP): is the product of the in phase voltage and current signals.

$$\begin{aligned} P = {} & \sum_{h=1}^{\infty} V_{ah}I_{ah}\ \cos(\theta_{ah} - \phi_{ah}) + \sum_{h=1}^{\infty} V_{bh}I_{bh}\ \cos(\theta_{bh} - \phi_{bh}) \\ & + \sum_{h=1}^{\infty} V_{ch}I_{ch}\ \cos(\theta_{ch} - \phi_{ch}) \end{aligned} \tag{29}$$

Effective Apparent Power (EAP): is composed of the active power and non active power, and it is equal to the product of the voltage by the current. It can be presented as:

$$S_e = 3V_eI_e \tag{30}$$

Voltage Distortion Power (VDP): the non fundamental apparent power consumed in a system is composed of the current distortion power, the voltage distortion power and the harmonic apparent power. The VDP is proportional to the product of the fundamental current with the harmonic voltage. It can be represented by the formula:

$$D_{eV} = 3\underbrace{\sqrt{V_e^2 - V_{e1}^2}}_{V_{eH}} I_{e1} \tag{31}$$

Harmonic Apparent Power (HAP): is a component of the non fundamental apparent power consumed in a system. It is proportional to the product of the harmonic voltage with the harmonic current.

$$S_{eH} = 3V_{eH}\underbrace{\sqrt{I_e^2 - I_{e1}^2}}_{I_{eH}} \tag{32}$$

Fundamental Positive Sequence Apparent Power (FPAP): apparent power is the square root of the squared sum of the active and reactive power consumed in a system. The fundamental positive sequence apparent power is the square root of the squared sum of the positive sequence active and reactive powers.

$$S_1^+ = 3\sqrt{\underbrace{[V_1^+ I_1^+ \cos(\theta_1^+ - \phi_1^+)]^2}_{\frac{P_1^+}{3}} + \underbrace{[V_1^+ I_1^+ \sin(\theta_1^+ - \phi_1^+)]^2}_{\frac{Q_1^+}{3}}} = 3V_1^+ I_1^+ \tag{33}$$

Load Unbalance Factor (LUF): is relate to the ratio of the fundamental apparent power to the fundamental positive sequence power. It provides a measure of how much power is produced due to the unbalance in a three phase system.

$$\frac{S_{U1}}{S_1^+} = \sqrt{\left(\frac{V_{e1}I_{e1}}{V_1^+ I_1^+}\right)^2 - 1} \tag{34}$$

Harmonic Pollution Factor (HPF): is the ratio of the non fundamental apparent power to the fundamental apparent power.

$$\frac{S_{eN}}{S_{e1}} = \sqrt{\left(\frac{S_e}{S_{e1}}\right)^2 - 1} = \sqrt{\left(\frac{V_e I_e}{V_{e1} I_{e1}}\right)^2 - 1} \tag{35}$$

6. Simulations

6.1. Simulation setup

The following simulations were run on a dell computer with 3 GB of RAM and an intel core 2 duo processor at 3 GHz. The aim of these simulations is to (a) show the trend between the error for calculating the phase and magnitude using the LS-ESPRIT and TLS-ESPRIT techniques versus the AMS and (b) to show the performance of the ESPRIT techniques compared to the FFT technique. A window length of 0.08 s is used for both methods and a 2048 point FFT was used in the computations of the WSA-WCSA. The sampling frequency was set to 3 kHz to accommodate the higher frequency; hence the window length is $N = 240$ points for both methods.

IEEE Std 1159 specifies that the noise level can be between 0 and 1% of the fundamental component. Further it can be understood from Tables 10.3–10.5 of the IEEE Std 519-1992 [10] that even harmonics are much smaller compared to the odd harmonic levels and harmonics beyond the harmonic number 21 are negligible. With this knowledge our simulation signal $s(t)$ contained odd harmonics up to the 21st order with a magnitude of $1/(2l+1)$ of the fundamental current amplitude (square wave) where $(2l+1)$ is the harmonic order and also it was injected with a Gaussian noise $w(t)$ with mean zero and variance of 1. The following equation shows the test signal in continuous time domain. Note ϕ_p is a random phase.

$$s(t) = \sum_{l=0}^{10} \underbrace{\frac{240}{(2l+1)}}_{h} \sin(2\pi \underbrace{(2l+1)}_{h} 50t + \phi_p) + w(t) \tag{36}$$

AMS's ranging from 25 to 35 for estimating the phase and magnitude errors were examined in line with the claim in Section 4.1. On the other hand for analyzing the computational cost, the AMS ranged from 11 to 35.

Finally the simulation was run several times and mean values were calculated for the errors and the computational time.

6.2. Simulation result discussion

In Figs. 2–3 the horizontal axis is the value for the AMS and the vertical axis is the PE using the ESPRIT-MA method. It can be seen from Figs. 2–3 that the PE for the magnitude and phase estimations for the harmonics drop around an AMS of 26. Considering that we have 11 real harmonics or 22 complex harmonics in our signals $22+4=26$ shows that 4 is a satisfactory number if we decide to consider harmonics up to this range. It has to be said that smaller number of harmonics will allow the constant c to be lower. Further it can be seen from Figs. 2–3 that both the TLS and LS-ESPRIT perform very closely in terms of accuracy.

Fig. 4 shows that the TLS algorithm is more expensive than the LS version of ESPRIT and the LS-ESPRIT performs better or approximately the same as the FFT based WSA-WCSA method in terms of computational cost for an AMS of approx 20 or less given 2048 FFT points. Given the practical situations discussed previously the cost of running the LS-ESPRIT would most likely be around 1.5 times that of the WSA-WCSA/FFT method.

7. Experiment

The VI's discussed above with and without the use of a KF were implemented in real time using Matlab Simulink [38] and DSPACE [39]. We chose the LS-ESPRIT technique over the TLS-ESPRIT as the accuracy of both techniques were very similar and further it was shown that the LS-ESPRIT had a better computational time when compared to the FFT method. A sampling frequency of 1 kHz was used. Also we chose a window length of 0.08 s ($N = 80$ samples) for the ESPRIT-MA method and a window of length 0.12 s ($N = 120$ samples) for the WSA-WCSA method. The AMS size was set to $n = 11$ in the ESPRIT-MA method due to the number of harmonics present. The reason for choosing this length for the WSA-WCSA method is because of accuracy, since smaller window sizes show significant errors in estimating the PQIs. Some explanation was provided in [21,22] and this can further be studied in books such as [36]. The test circuit is depicted in Fig. 5. A three-phase programmable power supply [40] with a line-to-line voltage of 382 volts was used to supply the power. Further harmonics 3 at 33%, 5 at 20% and 7 at 14.28% of the fundamental was injected into the system. Like the simulation these harmonics were chosen purposefully as they are the first 7 odd harmonics in a square wave. Data was obtained on the RL circuit over a period of several seconds.

All the important PQIs stated in the IEEE Standard 1459 and discussed in Section 5 were computed and the results are tabulated in Tables 1–2. Table 1 presents the PE of the estimation from the calculated true values for the PQIs detailed in Section 5. Table 2 shows the variance in the PE. Moreover there are two rows for each

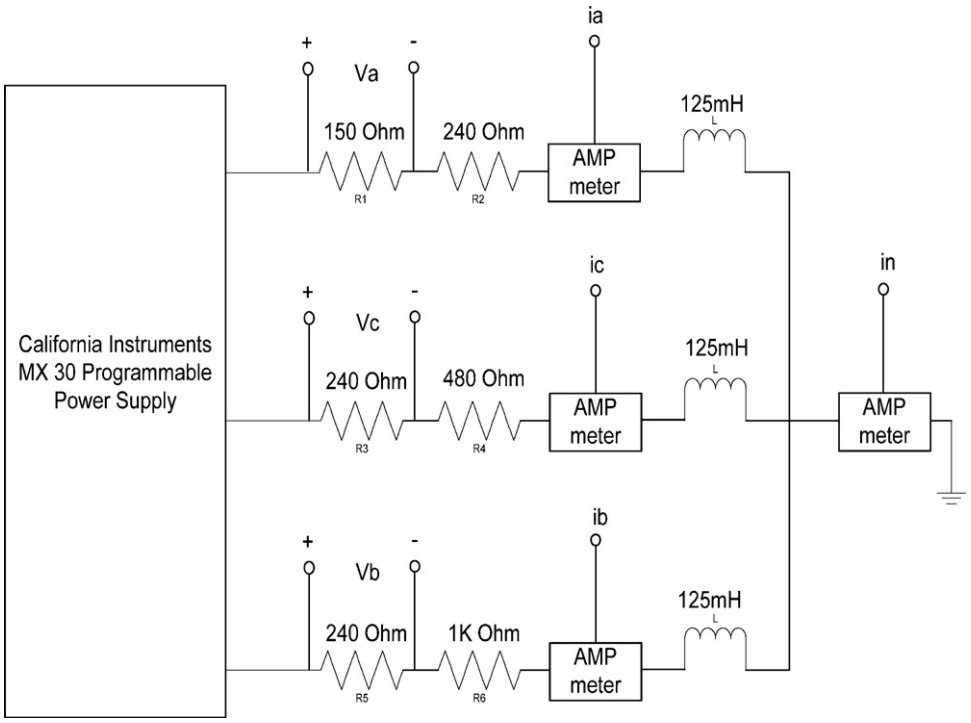

Fig. 5. Experiment circuit diagram.

PQI. The first row shows the results for the KF VI, the second row shows the results with *No Kalman Filtering* for the VI (NKF VI).

Finally the windows examined are the *Bartlett window* (BW), *Blackman window* (BLW) and the *Hamming window* (HMW) more details on these windows can be found in [33]. Each column in the table indicates the results obtained for each of the methods (ESPRIT-MA or WSA-WCSA) and the WT used (BW, BLW and HMW).

8. Discussion of results

The VI using the KF performed similar to the VI without the KF (NKF VI) using the ESPRIT-MA technique. Their absolute difference was less than 1%, but the variance was reduced by many orders of the magnitude (bigger than 10 times). The NKF VI based on the ESPRIT-MA technique had an overall average error of 3.0% for the PQIs estimations while the NKF VI based on WT, averaged at 2.2%, 2.5% and 2.6% for the PQIs estimations for the BW, BLW, and HMW respectively. The estimation error for the KF VI based on the ESPRIT-MA technique was 2.9% while that for the WTs were 2.2%, 2.5% and 2.5% for the BW, BLW, and HMW, respectively. Fig. 6 below indicates these trends graphically.

It can be realized that the ESPRIT-MA based technique performed very close to the other WTs with the overall PQIs estimation error difference between the ESPRIT-MA and the best WT method used in WSA-WCSA being 0.83% for the VI with NKF and 0.60% for the VI using the KF.

Table 1
Percentage error for various PQIs using the subspace and WSA-WCSA method.

PQI	ESPRIT	BW	BLW	HMW
LUF	1.4278	2.1603	4.2641	4.8799
	1.0418	2.4882	4.4306	4.7798
HPF	3.6298	3.5813	3.5696	3.7288
	3.5896	3.5767	3.6196	3.7091
EAP	2.3841	1.97	1.8138	1.9736
	2.387	1.959	1.822	1.9613
ACP	3.5781	3.3062	3.2321	3.4038
	3.5763	3.3055	3.233	3.4039
FPAP	4.527	0.7066	1.4412	1.862
	4.1984	0.34014	1.5963	1.7542
FPRP	3.5223	1.6569	3.9355	3.6451
	3.0306	1.8348	4.039	3.2614
FPPF	0.81658	1.9138	2.0921	1.5105
	0.89331	1.7941	1.9844	1.2798
FPACP	5.3502	2.5949	0.77804	0.62878
	5.1427	2.1441	0.43187	0.49997
VDP	3.1481	2.7814	2.5204	2.6883
	3.1401	2.7821	2.5224	2.6917
HAP	2.0522	1.6175	1.5071	1.6632
	2.0591	1.6185	1.513	1.6611

Table 2
Variance in the percentage error for various PQIs using the subspace and WSA-WCSA method.

PQI	ESPRIT	BW	BLW	HMW
LUF	0.018039	0.01646	0.013509	0.011959
	0.63101	0.23073	0.35351	0.33703
HPF	0.00023	3.10E-05	0.001058	0.000552
	0.066394	1.81E-02	0.038351	0.028987
EAP	0.023889	0.012286	0.015763	0.011599
	0.038734	0.016201	0.028101	0.01836
ACP	0.009317	0.000793	0.005455	0.000732
	0.026604	0.00663	0.019369	0.005503
FPAP	0.01844	0.016636	0.012788	0.011607
	0.81157	0.17489	0.30482	0.27765
FPRP	0.033596	0.004568	0.01202	0.046194
	0.87704	0.47157	0.61814	0.90506
FPPF	0.001073	0.00238	0.002702	0.009278
	0.24713	0.15983	0.22118	0.339
FPACP	0.010568	0.032131	0.013735	0.003485
	1.4832	0.391	0.31193	0.23379
VDP	0.022218	0.005478	0.013145	0.005326
	0.038116	0.009863	0.020079	0.010423
HAP	0.03031	0.019392	0.03072	0.023992
	0.05302	0.024875	0.041704	0.031532

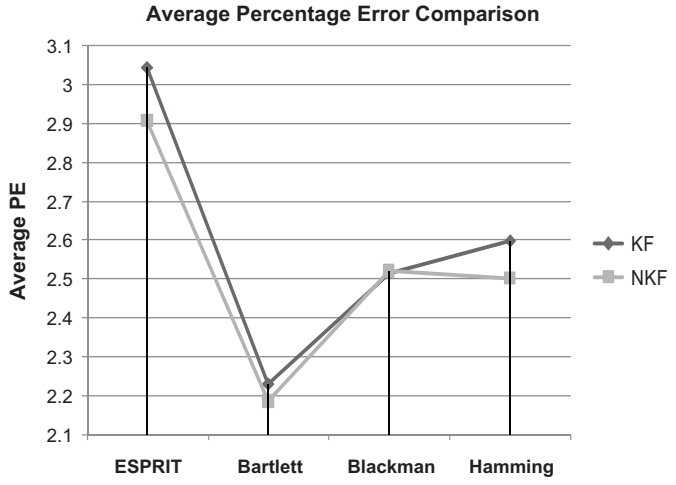

Fig. 6. Overall average PE in estimating PQIs.

9. Conclusion

In this paper we showed a VI using the LS-ESPRIT technique and MA with a KF to compute the PQIs as defined in IEEE Std 1459-2010. The ESPRIT-MA VI proved to be accurate in estimation compared to the WSA-WCSA which uses the FFT method. Also it proved to be efficient in computational requirements given real situations. It is good to emphasize that the ESPRIT and MA method is capable of estimating the PQIs with fewer cycles of the power signal, which is not possible with the WT methods. Finally the ESPRIT-MA based techniques were shown to be good in estimating inter-harmonics and other PQ issues; this was presented in other technical literature referenced in the introduction of this article. With the ever growth of processor speed and in the same time the reduction in their prices, subspace methods have the potential to be very promising tools for the PQ industry.

Potential future work can include finding more robust/efficient ways for estimating the phase and magnitude using the subspace methods and an efficient way of estimating the number of frequency components in a PS signal.

References

[1] W.G. Morsi, M.E. El-Hawary, Power quality evaluation in smart grids considering modern distortion in electric power systems, Electr. Pow. Syst. Res. 81 (2011) 1117–1123.
[2] D. Jakus, R. Goic, J. Krstulovic, The impact of wind power plants on slow voltage variations in distribution networks, Electr. Pow. Syst. Res. 81 (2011) 589–598.
[3] M.H. Albadi, E.F. El-Saadany, Overview of wind power intermittency impacts on power systems, Electr. Pow. Syst. Res. 80 (2010) 627–632.
[4] S. Mujovic, V.A. Katic, J. Radovic, Improved analytical expression for calculating total harmonic distortion of PC clusters, Electr. Pow. Syst. Res. 81 (2011) 1317–1324.
[5] J.M.C. Filho, R.C. Leborgne, P.M. da Silveira, M.H.J. Bollen, Voltage sag index calculation: comparison between time-domain simulation and short-circuit calculation, Electr. Pow. Syst. Res. 78 (2008) 676–682.
[6] M. Khederzadeh, Mitigation of the impact of transformer inrush current on voltage sag by TCSC, Electr. Pow. Syst. Res. 80 (2010) 1049–1055.
[7] M.S. Azam, T. Fang, K.R. Pattipati, R. Karanam, A dependency model-based approach for identifying and evaluating power quality problems, IEEE Trans. Power Deliver. 19 (2004) 1154–1166.
[8] IEEE, IEEE Standard Definitions for the Measurement of Electric Power Qualities Under Sinusoidal, Nonsinusoidal, Balanced, or Unbalanced Conditions, 2010.
[9] IEEE, IEEE Recommended Practice for Monitoring Electric Power Quality, 2009.
[10] IEEE, IEEE Recommended Practices and Requirements for Harmonic Control in Electrical Power Systems, IEEE Std 519-1992, 1993, pp. 0–1.
[11] IEC, Electromagnetic compatibility (EMC). Part 3.2: Limits – limits for harmonic current emissions (equipment input current < 16 A per phase), 2007.
[12] IEC, Electromagnetic compatibility (EMC). Part 3.12: Limits – limits for harmonic currents produced by equipment connected to public low-voltage systems with input current > 16 A and <75 A per phase, 2006.
[13] IEC, Electromagnetic compatibility (EMC). Part 3.4: Limits – limitations of emission of harmonic currents in low-voltage power supply systems for equipment with rated current greater than 75A, 2007.
[14] A. Alkan, A.S. Yilmaz, Frequency domain analysis of power system transients using Welch and Yule-Walker AR methods, Energy Convers. Manage. 48 (2007) 2129–2135.
[15] Q. Hao, Z. Rongxiang, C. Tong, Interharmonics analysis based on interpolating windowed FFT algorithm, IEEE Trans. Power Deliver. 22 (2007) 1064–1069.
[16] G.W. Chang, C.I. Chen, Y.J. Liu, M.C. Wu, Measuring power system harmonics and interharmonics by an improved fast fourier transform-based algorithm, generation, transmission & distribution, IET 2 (2008) 193–201.
[17] A. Testa, D. Gallo, R. Langella, On the processing of harmonics and interharmonics: using Hanning window in standard framework, IEEE Trans. Power Deliver. 19 (2004) 28–34.
[18] A.A. Girgis, F.M. Ham, A quantitative study of pitfalls in the FFT, IEEE Trans. Aerosp. Syst. AES-16 (1980) 434–439.
[19] Z. Fusheng, G. Zhongxing, Y. Wei, The algorithm of interpolating windowed FFT for harmonic analysis of electric power system, IEEE Trans. Power Deliver. 16 (2001) 160–164.
[20] Ö. Salor, Spectral correction-based method for interharmonics analysis of power signals with fundamental frequency deviation, Electr. Power Syst. Res. 79 (2009) 1025–1031.
[21] R. Zolfaghari, Y. Shrivastava, V.G. Agelidis, Spectral analysis techniques for estimating power quality indices, in: 14th International Conference on Harmonics and Quality of Power (ICHQP), 2010, pp. 1–8.
[22] R. Zolfaghari, Y. Shrivastava, V.G. Agelidis, G.M.L. Chu, Spectral analysis techniques with Kalman filtering for estimating power quality indices, in: IEEE PES Innovative Smart Grid Technologies Conference Europe (ISGT Europe), 2010, pp. 1–8.
[23] R. Roy, T. Kailath, ESPRIT-estimation of signal parameters via rotational invariance techniques, IEEE Trans. Acoust. Speech Signal Process. 37 (1989) 984–995.
[24] R. Roy, A. Paulraj, T. Kailath, ESPRIT – a subspace rotation approach to estimation of parameters of cisoids in noise, IEEE Trans. Acoust. Speech Signal Process. 34 (1986) 1340–1342.
[25] R. Schmidt, Multiple emitter location and signal parameter estimation, IEEE Trans. Antennas Propag. 34 (1986) 276–280.
[26] Z. Leonowicz, T. Lobos, Parametric spectral estimation for power quality assessment, in: The International Conference on Computer as a Tool, EUROCON, 2007, pp. 1641–1647.
[27] P. Tripathy, S.C. Srivastava, S.N. Singh, A modified TLS-ESPRIT-based method for low-frequency mode identification in power systems utilizing synchrophasor measurements, IEEE Trans. Power Syst. PP (2010) 1.
[28] I.Y.H. Gu, M.H.J. Bollen, Estimating interharmonics by using sliding-window ESPRIT, IEEE Trans. Power Deliver. 23 (2008) 13–23.
[29] A. Bracale, G. Carpinelli, Z. Leonowicz, T. Lobos, J. Rezmer, Measurement of IEC groups and subgroups using advanced spectrum estimation methods, IEEE Trans. Instrum. Meas. 57 (2008) 672–681.
[30] A. Bracale, G. Carpinelli, D. Lauria, Z. Leonowicz, T. Lobos, J. Rezmer, On some spectrum estimation methods for analysis of nonstationary signals in power systems. Part I. Theoretical aspects, in: 11th International Conference on Harmonics and Quality of Power, 2004, pp. 266–271.
[31] A. Bracale, G. Carpinelli, D. Lauria, Z. Leonowicz, T. Lobos, J. Rezmer, On some spectrum estimation methods for analysis of nonstationary signals in power systems. Part II. Numerical applications, in: 11th International Conference on Harmonics and Quality of Power, 2004, pp. 260–265.
[32] R. Zolfaghari, Y. Shrivastava, V.G. Agelidis, G.M.L. Chu, Using windowed ESPRIT spectral estimation for measuring power quality indices, in: 2010 IEEE PES Innovative Smart Grid Technologies Conference Europe (ISGT Europe), 2010, pp. 1–8.
[33] F.J. Harris, On the use of windows for harmonic analysis with the discrete Fourier transform, Proc. IEEE 66 (1978) 51–83.
[34] D.G. Manolakis, V.K. Ingle, S.M. Kogon, Statistical and adaptive signal processing: spectral estimation, signal modeling, adaptive filtering and array processing, McGraw-Hill, Boston, 2000.
[35] C.F.V.L. Gene H, Golub Matrix Computations, third ed., Johns Hopkins, 1996.
[36] D.G.M.J.G. Proakis, Digital Signal Processing, Principles Algorithms and Applications, fourth ed., Prentice Hall, 2005.
[37] B. Ottersten, M. Viberg, T. Kailath, Performance analysis of the total least squares ESPRIT algorithm, IEEE Trans. Signal Process. 39 (1991) 1122–1135.
[38] Mathworks and Simulink.
[39] DSpace Technologies.
[40] California Instruments.